

The Properties (Rheological, Dielectric, and Mechanical) and Microtopography of Spherical Fullerene-Filled Poly(arylene ether nitrile) Nanocomposites

Wei Yang, Xulin Yang, Zejun Pu, Mingzhen Xu, Xiaobo Liu

Research Branch of Functional Materials, Institute of Microelectronic and Solid State Electronic, High-Temperature Resistant Polymers and Composites Key Laboratory of Sichuan Province, University of Electronic Science and Technology of China, Chengdu 610054, People's Republic of China

Correspondence to: Xiaobo Liu (E-mail: Liuxb@uestc.edu.cn)

ABSTRACT: Poly (arylene ether nitrile)/fullerene (PEN/fullerene) nanocomposites were prepared by a facile solution-cast method and the rheological, dielectric, mechanical, and morphological properties of the resulted nanocomposites were systematically studied and compared. Rheological studies showed PEN/fullerene nanocomposites percolation network formed at fullerene containing of 1.50 wt %, when the shear frequency was fixed at 0.1 Hz, the fitted rheological percolation threshold was about 1.55 wt %, very close to the experimental observations. The dielectric transition occurs when the fullerene loading reached 1.50 wt %, that is very close to its rheological percolation threshold. At this point, PEN/fullerene nanocomposites also showed the optimal mechanical properties with a tensile strength of 93.6 MPa and modulus of 1951.5 MPa, which is increased by 27% and 15% compared with the pure PEN. SEM and TEM images have manifested the separate fullerene aggregated to fullerene bundles in PEN/fullerene nanocomposites, and the dispersion of fullerene bundles begin to go bad when the containing above 1.50 wt %. The PEN/fullerene nanocomposites can be widely used due to its excellent dielectric and mechanical performance. © 2013 Wiley Periodicals, Inc. *J. Appl. Polym. Sci.* **2014**, *131*, 40100.

KEYWORDS: rheology; nanostructured polymers; dielectric properties; viscosity and viscoelasticity; mechanical properties

Received 6 June 2013; accepted 20 October 2013

DOI: 10.1002/app.40100

INTRODUCTION

Because of the size and surface effect of nanoparticles, nanoparticles-based polymer nanocomposites with multifunctional properties have recently attracted tremendous researches.^{1–4} The properties of polymer/nanoparticles nanocomposites can be more greatly improved than those of conventional composites and polymer nanocomposites are considered as the most promising materials that can be widely used in advanced fields such as medicals, electronics, water purification, aerospace.⁵

To date, nanocarbons of quasi-one-dimensional carbon nanotube (CNT) and two-dimensional graphene nanosheet (GN) have been mostly used to prepare polymer nanocomposites and their mechanical, thermal, electrical, morphological, especially dielectric, and rheological properties were studied. Numerous studies have indicated that CNT and GN are surely ideal fillers to prepare high dielectric constant polymer materials. In addition, the general results found that there is a dielectric transition regarding GN, which is usually larger than the rheological percolation threshold, but for CNT the dielectric transition has not been observed. For example, Fan et al. found the rheological percolation threshold

for PVDF/GN nanocomposites is 0.0018 vol % smaller than the dielectric transition value (0.0177 vol %).^{6,7} For CNT-filled nanocomposites, the dielectric constant or electrical conductivity constantly increasing with the increase of CNT loading.⁸

On the contrary, zero-dimensional fullerene with a special hollow cage structure can be used to prepare low dielectric constant materials.^{9,10} However, there is little report on the rheological properties of polymer/fullerene systems. Thus, it should be studied to understand the filler effect of zero-dimensional fullerene in polymer matrix and to further expand the application of polymer/fullerene nanocomposites.

Poly (arylene ether nitrile) (PEN) is the main polymer host since it exhibits excellent mechanical strength, high temperature resistance, strong chemical inertia.^{11–14} Those properties, together with its excellent dielectric performance makes it good polymer matrices for dielectric materials. On the other hand, Chen et al. used toluene/*N*-methyl pyrrolidone double-solution-cast method to obtain fullerene-doped PEN films.¹⁵ However, the dielectric properties of pure PEN based on various monomers such as hydroquinone (HQ), resorcinol (RS), bisphenol

A (BPA), phenolphthalein (PP), and phenolphthalein (PPL) varied a lot. The polar groups on the PP-based PEN the authors used are disadvantageous to lower dielectric constant. In addition, fullerene may first float on the surface of the film as toluene volatiles, which is detrimental to the fullerene dispersion in the films. Moreover, the dielectric constant and loss of the obtained films fluctuated as fullerene is from 2 to 5% while the reason is unknown.

Thus in this study, completely symmetrical BPA-based PEN was employed and PEN/fullerene nanocomposites were prepared by a solution-cast method via continuous supersonic technology. Their dielectric, mechanical and rheological properties as well as the morphological were thoroughly studied and compared. This paper not only studied the structure (dispersion, interaction, percolation) and property, but also shows that rhetorical transition is close to dielectric transition value in the spherical fullerene-filled polymer material.

EXPERIMENT

Materials

Bisphenol A-based polyarylene ether nitrile (PEN) with the density of 1.2 g/cm³ and the inherent viscosity of 1.21 dL/g (0.005 g/mL in *N*-methylpyrrolidone) was purchased from Sichuan FEIYA new material co., LTD in Guangyuan, China. fullerene (the mixture of C₆₀ and C₇₀) was provided by China Rubber Group Carbon Black Research & Design Institute in Zigong, China. *N*-Methyl pyrrolidone (NMP) was purchased from Kelong Chemicals in Chengdu, China.

Preparation of PEN/Fullerene Nanocomposite Films

The preparation of PEN/fullerene nanocomposites was generally as follows. First, a weight-measured of fullerene (0.00 wt % to 3.00 wt %) was added in NMP and sonication in water bath for 1 h. Meanwhile; a certain content of PEN was dissolved in NMP with a mechanical stir. The mixture was refluxed at 200°C for 10 min after PEN was totally dissolved. Second, first-ultrasonic fullerene was added to PEN and mixed under sonication for 1 h. The mixture was then put on a clean preheated glass plate and cast solvents using a sequential mode of temperature program at 80, 100, 120, 160°C for 1 h, and at 200°C for 2 h. Then it was cooled to room temperature gradually, the PEN/fullerene nanocomposite films were thus obtained.

Measurements

The rheological measurements were carried out using rheometer (Rheometer AR-G2, TA Instruments) equipped with parallel-plate geometry (25 mm diameter). Samples with a thickness of 1.0 mm and diameter of 25 mm were melted at 320°C for 3 min in the parallel-plate fixture before measurements. Dynamic strain sweep measurements were firstly conducted to determine the linear viscoelastic region.^{16,17} The strain sweep scans were carried out between 0.1% and 100% at 300, 320, and 340°C. Frequency sweeps were conducted from 0.1 to 100 Hz with a strain of 1%, at 320°C.

Differential scanning calorimetry (DSC) analysis was measured on TA instrument DSC Q100, under N₂ atmosphere at a heating rate of 10°C/min. All reported data were obtained from a second heating cycle.

Dielectric properties of the films were monitored on a TH2819A instrument of Tonghui, China from 50 Hz to 200 KHz at 25°C. For sample preparation, the nanocomposite films were cut into small pieces (length: 10 mm; width: 10 mm and thickness: 110~130 μm), and coated with conductive silver paste on both surfaces and dried at 80°C for 30 min.^{15,18,19} The final results were the average values of three replicate measurements.

Mechanical properties of the pure PEN and PEN/fullerene nanocomposites were tested by a SANS CMT6104 series desktop electromechanical universal testing machine (Shenzhen, China), with the sample size followed the IV standard of GB 13022-91(strip-type, width 10 mm, overall length 160 mm, gauge length 100 mm) and at a stretching speed of 5 mm/min. The final results were the average values of five replicate measurements.

The cross section morphology of the films was observed on SEM (JSM-5900 LV) operating at 5.0 kV, prior to be tested the samples were cryo-fractured by liquid nitrogen and coated with a thin layer of gold prior to examination. The dispersion of fullerene in PEN matrix was observed on TEM (JEM-2100F) operating at 200.0 kV, samples for the text were cut into about 80 nm by the frozen ultrathin sections instrument (EM UC7/FC7).

RESULTS AND DISCUSSION

Rheological Properties of PEN and PEN/Fullerene Nanocomposites

The dynamic strain sweep is first conducted to determinate the linear viscoelastic region of the pure PEN and PEN/fullerene nanocomposites. The sweep curves of pure PEN under 300, 320, 340°C are shown in Figure 1(a). The linear region shifts to much higher strain values when temperature shifts from 300°C to 320°C, but the curve at 320°C is similar to the one at 340°C. Thus, the latter rheological tests were conducted at 320°C. The sweep curves of pure PEN and PEN/fullerene nanocomposite containing 3 wt % fullerene (PEN/fullerene3.0) at 320°C are shown in Figure 1(b). It can be observed that the two curves are relatively flat at first. With the increasing of strain to 10%, the storage modulus (G') of PEN/fullerene3.0 tends to decrease, indicating the linear viscoelastic region starts to disappear. In addition, the deviation from linear behavior for PEN/fullerene composites occurs at the strain about 10.5%, which is less than that of the pure PEN (about 20%). Therefore, subsequent dynamic frequency scan measurements were conducted at a strain of 1% and temperature of 320°C. In other reports, the deviation from linear behavior for PEN/GN and PEN/CNT nanocomposites occurs at a strain of about 1–2%^{17,18} and 14%,²⁰ respectively, indicating that PEN/fullerene composites are less sensitive to the strain than PEN/GN nanocomposites but more sensitive to the strain than PEN/CNT nanocomposites. It should also be noted that the addition of fullerene changed the storage modulus of PEN, the G' for PEN/fullerene3 is much higher than that of the pure PEN.

The G' and loss modulus (G'') for pure PEN and PEN/fullerene nanocomposites are shown in Figure 2(a,b), respectively. At low frequencies, the G' increased significantly when the 0.25 wt % fullerene were added into PEN (PEN/Fullerene0.25). In

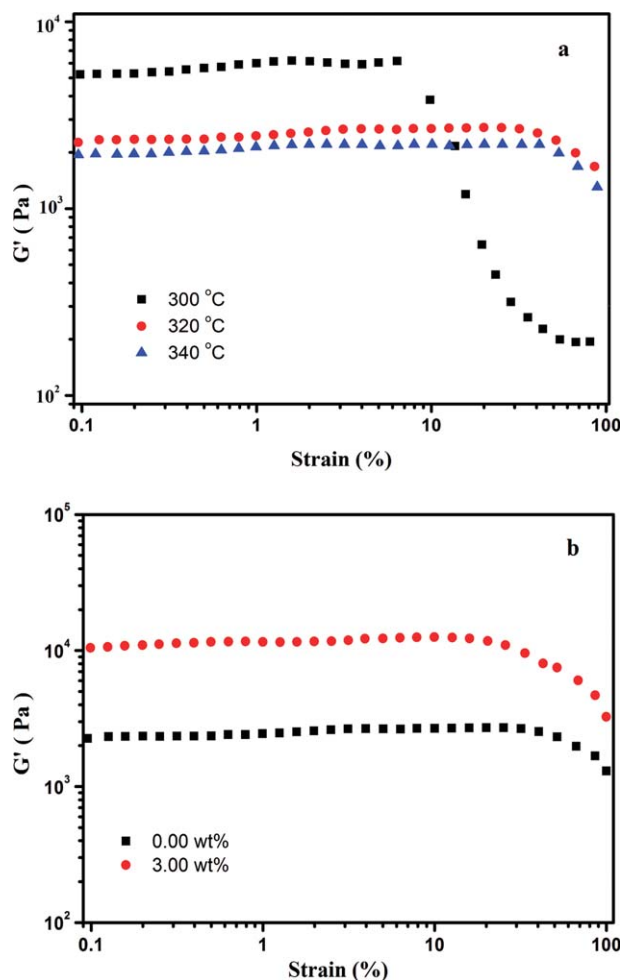


Figure 1. (a) storage modulus (G') for pure PEN obtained in dynamic strain sweeps at 300, 320, and 340 °C, (b) G' for pure PEN and PEN/fullerene-3.0 nanocomposites obtained in dynamic strain sweeps at 320 °C. [Color figure can be viewed in the online issue, which is available at wileyonlinelibrary.com.]

addition, the frequency dependence of G' and for PEN/Fullerene-0.25 is quite different from that of pure PEN. Then, the G' slightly increases and almost keeps the same values below 1.50 wt %. However, when fullerene content exceeds 1.50 wt %, the G' increases sharply and showed little frequency dependence. Namely, at the low frequencies the PEN/fullerene nanocomposites experiences a terminal plateau as the fullerene content reached a critical value about 1.50 wt %, and PEN/fullerene nanocomposites may experience a transition from liquid-like behavior to solid-like one.¹⁵ With the increase of frequency, a terminal plateau occurred for all PEN/fullerene nanocomposites and all G' tend to be overlapped. That may attribute to the material microstructure failure caused by high shear frequency. In Figure 2(b), the increase of G'' is much lower than that of the G' , indicating that in the PEN matrix the effect of fullerene on rheological behaviors is more sensitively reflected on the G' than on the G'' .^{17,18}

Figure 3 shows complex viscosity (η^*) of pure PEN and PEN/fullerene nanocomposites with different fullerene contents. At

low frequencies, the η^* of pure PEN shows little frequency dependence and almost behaves like a Newtonian fluid, since polymer chain is fully relaxed in all frequencies. Then, as the frequency goes, the η^* of neat PEN showed a shear thinning behavior. However, even a small addition of fullerene (0.25 wt %) into PEN makes Newtonian fluid behavior became small. Especially when fullerene content exceeds 1 wt %, Newtonian plateau has disappeared and a strong shear thinning behavior could be observed.

In addition, at low frequencies, the magnitude of η^* monotonically increases with the increasing fullerene loading, indicating that the large scale polymer relaxations are restrained by the presence of fullerene particles effectively,²¹ since polymer chains are partly adsorbed on the fullerene and partly entangled with neighboring one. When the fullerene loading is above 1.50 wt %, the trend of η^* becomes flat. That is because the restriction effect of fullerene on polymer chains tends to become saturation. Namely, a rheological percolation network has been formed when the fullerene loading is 1.50 wt %. Another reason

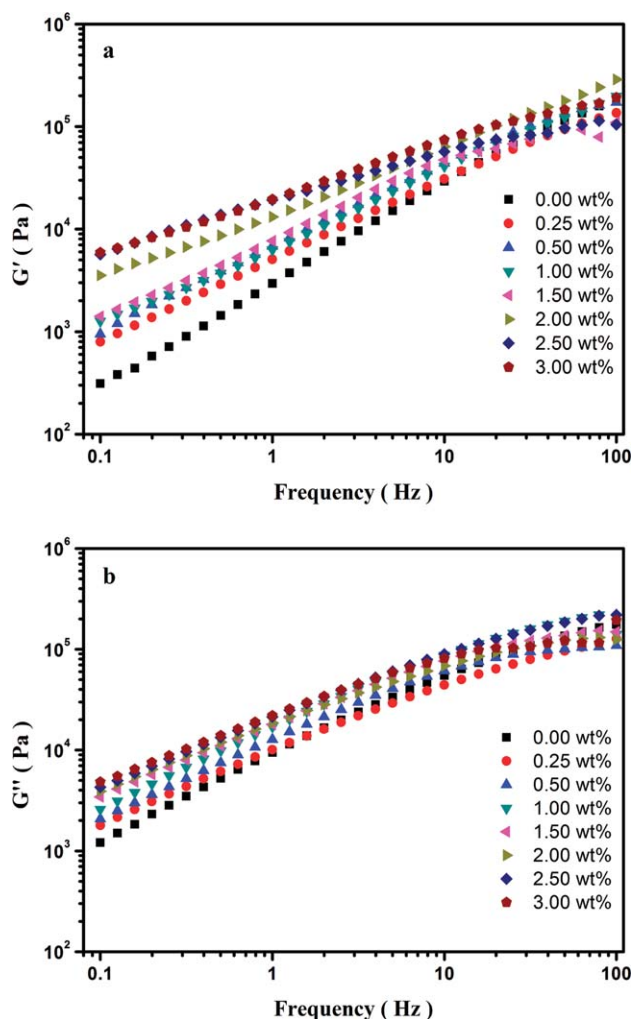


Figure 2. (a) storage modulus (G'), (b) loss modulus (G''), for pure PEN and PEN/fullerene nanocomposites at 320 °C. [Color figure can be viewed in the online issue, which is available at wileyonlinelibrary.com.]

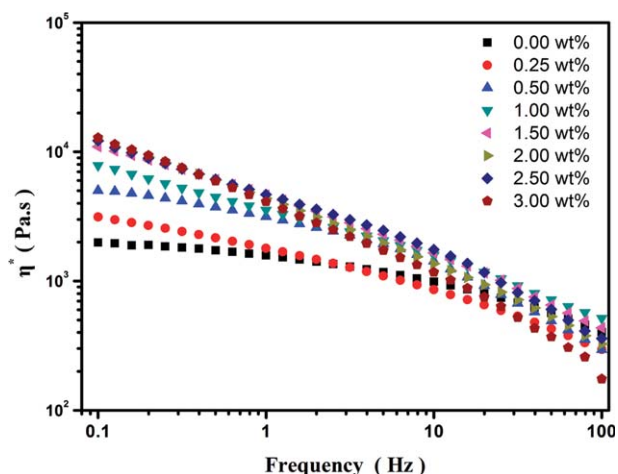


Figure 3. Complex viscosity (η^*) for pure PEN and PEN/fullerene nanocomposites at 320°C. [Color figure can be viewed in the online issue, which is available at wileyonlinelibrary.com.]

is that fullerene may be partially aggregated when fullerene loading is over 1.50 wt %.

Cole–Cole plots are usually used for the description of viscoelastic properties of those materials with a relaxation time distribution such as heterogeneous polymeric systems.^{22–24} To further understand the rheological behaviors of PEN/fullerene nanocomposites, Figure 4 shows Cole–Cole plots of imaginary viscosity (η'') vs. real viscosity (η') for the pure PEN and PEN/fullerene nanocomposites.

The relaxation plot of pure PEN obviously presented as an arc with a rigid tail on the right-hand side, indicates there are two relaxation mechanism. The arc represents relaxation process with a relaxation time distribution, and the rigid tail indicates the long-term relaxation of those PEN chains.²² In the PEN/fullerene-0.25, the radian of arc becomes larger and the rigid tail becomes longer than the pure PEN, indicating that the long-term

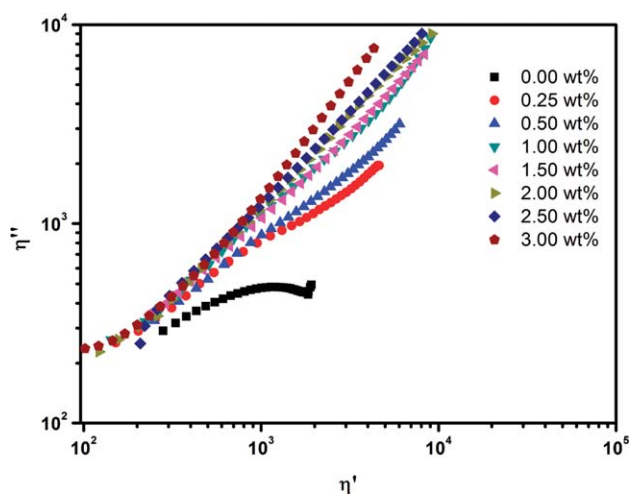


Figure 4. Cole–Cole plots of imaginary viscosity (η'') vs. real viscosity (η') for the pure PEN and PEN/fullerene nanocomposites at 320°C. [Color figure can be viewed in the online issue, which is available at wileyonlinelibrary.com.]

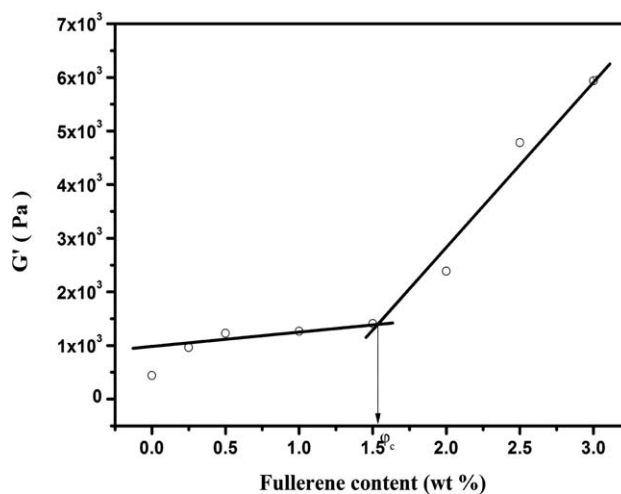


Figure 5. Storage modulus (G') as a function of the fullerene loading at 0.10 Hz and 320°C.

relaxation of those restrained PEN chains becomes stronger. With the increasing of fullerene loading the radian of arc and the length of the rigid tail also increased, and the upturn between these two parts presents remarkable shift to the higher viscosity region. When the fullerene loading reached 1.50 wt %, the arc almost disappeared, and the plot of PEN/fullerene-1.5 presented as a straight line, indicating that the long-term relaxation of those restrained PEN chains becomes the dominant one in the whole relaxation behaviors of the composites, and percolation network forms at present fullerene loadings.²² With the increase of fullerene loading, the relaxation plots of PEN/fullerene presented as bend upwards curves, demonstrating fullerene are excessive for the network. The Cole–Cole plots indicates fullerene particles retarded the relaxation process of the polymer chains in the molten state of and reduce the relax ability for the system strongly.^{16,22}

Figure 5 shows the relationship between G' of PEN/fullerene nanocomposites and fullerene loading at 0.1 Hz. Clearly, G' increases steadily as fullerene content goes. When fullerene

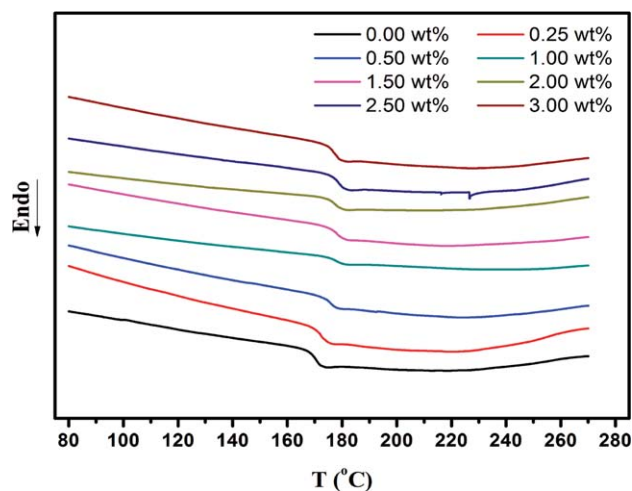


Figure 6. The DSC curves of pure PEN and PEN/fullerene nanocomposites at a scanning rate of 10°C/min. [Color figure can be viewed in the online issue, which is available at wileyonlinelibrary.com.]

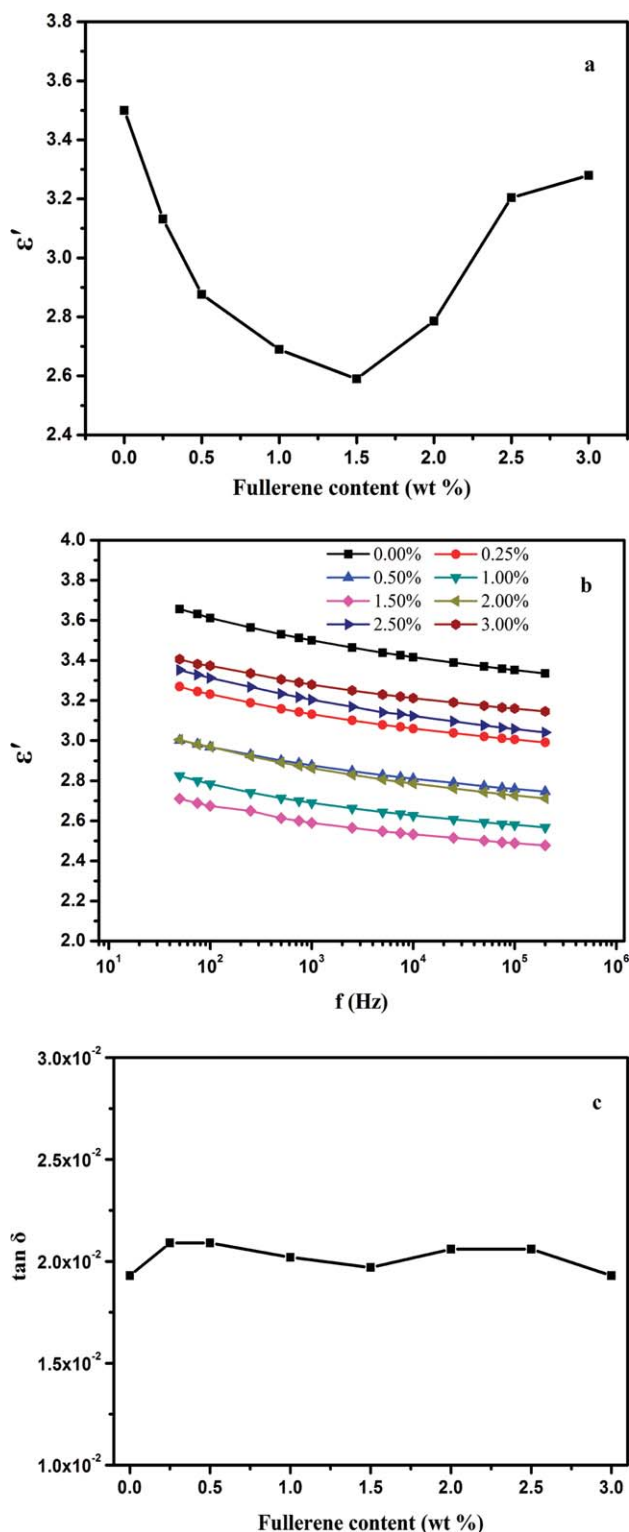


Figure 7. (a) the dielectric constant (ϵ'); (b) the variation of the dielectric constant with frequency; (c) the dielectric loss tangent value ($\tan \delta$), for the PEN and PEN/fullerene nanocomposites at 1 KHz and 25°C. [Color figure can be viewed in the online issue, which is available at wileyonlinelibrary.com.]

content is over 1.50 wt %, G' increases sharply, indicating that there is a sudden change in the material microstructure structure. At this loading level, the fullerene formed a rheological percolation network structure and highly hinders the large scale motion of polymer chains.²⁵ Figure 5 also gives that the fitted rheological percolation threshold is about 1.55 wt %, which is very close to the experimental observations. In the same PEN matrix, the reported rheological percolation for CNT is over 2 wt %²⁵ and for GN is about 0.8~1 wt %.¹⁸ Those rheological percolation differences may be due to their different dimensions and filler-polymer interactions.

DSC Analysis

To further confirm the PEN is restrained by the fullerene, DSC scans of pure PEN and PEN/fullerene nanocomposites were taken at a scanning rate of 10°C/min, as presented in Figure 6. The glass transition temperature (T_g) of pure PEN is at about 168°C and the T_g gradually increases but the heat capacity decrease (ΔC_p) decreasing with the increase of fullerene content when below 1.00 wt %. The T_g and ΔC_p reached their maximum (about 176.5°C) and minimum respectively at 1.00 wt %. Then, the T_g gradually decreasing and the ΔC_p increases when fullerene

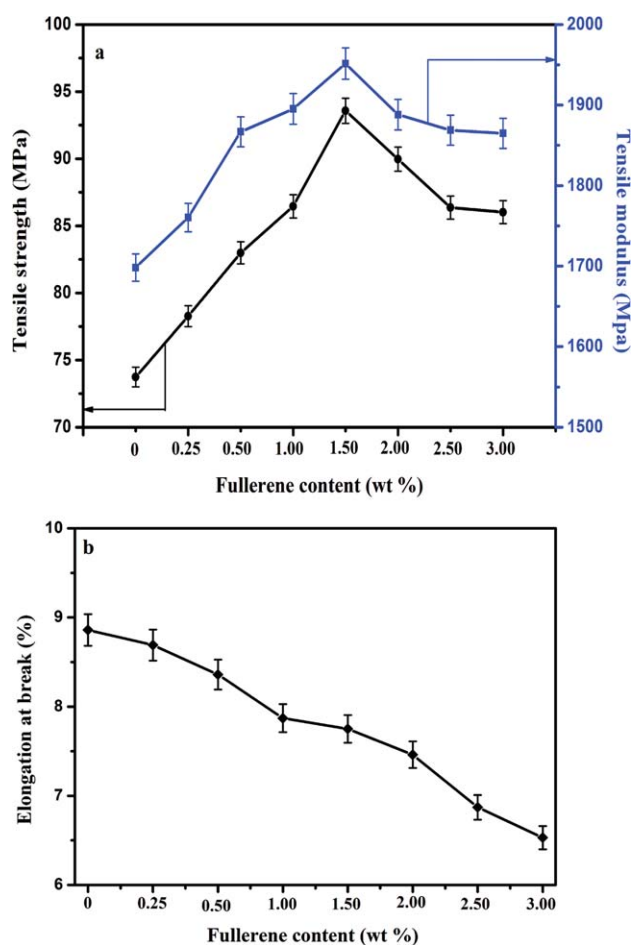


Figure 8. Mechanical properties of pure PEN and PEN/fullerene nanocomposites: (a) tensile strength and tensile modulus; (b) elongation at break. [Color figure can be viewed in the online issue, which is available at wileyonlinelibrary.com.]

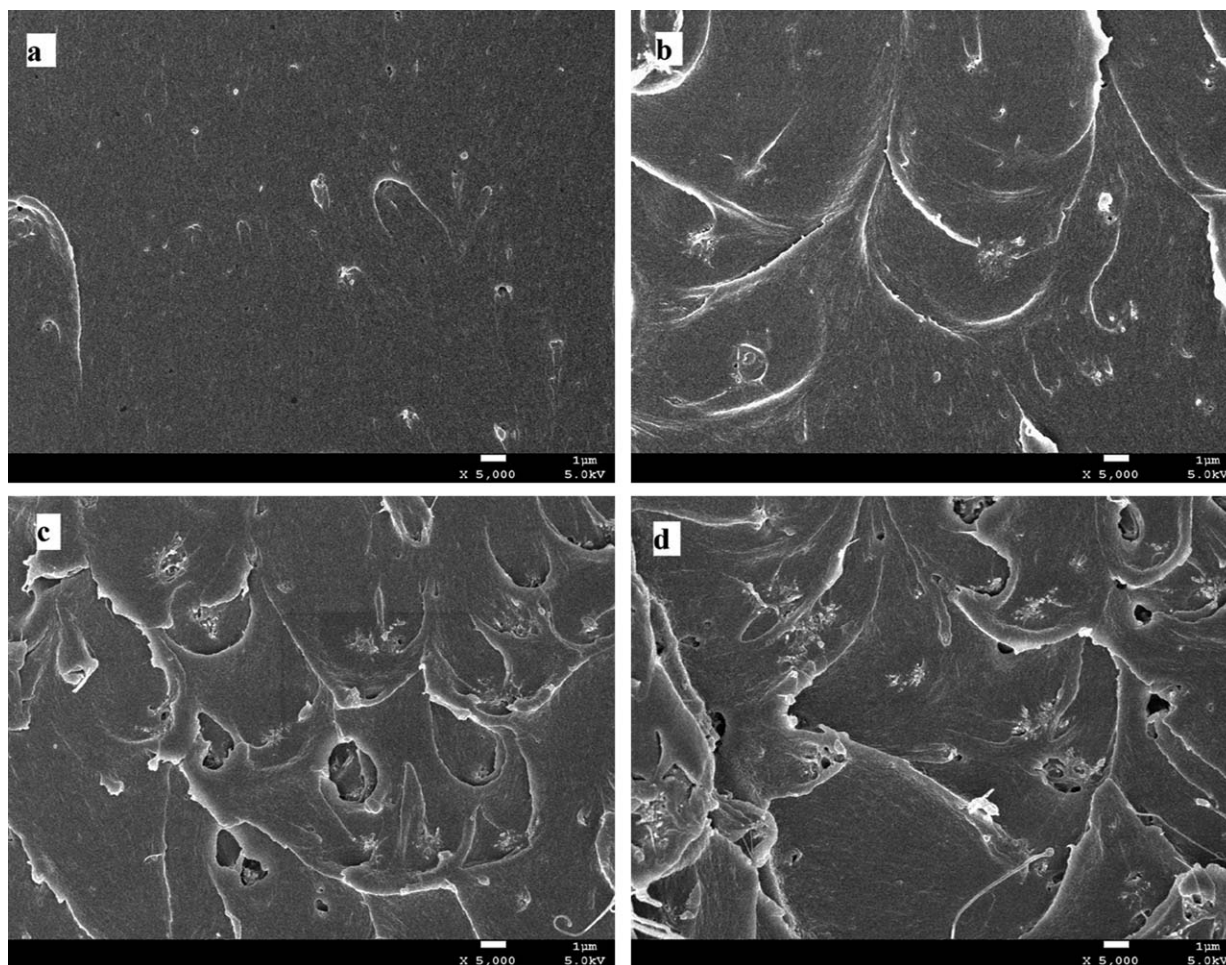


Figure 9. SEM pictures of fractured morphologies of (a) pure PEN; (b) PEN/Fullerene0.5; (c) PEN/Fullerene1.5; (d) PEN/Fullerene3.0.

content above 1.00 wt %, but even at 3.00 wt % the T_g (about 171°C) still higher and ΔC_p still smaller than the pure PEN.

The increasing of T_g and decreasing of ΔC_p below 1.00 wt % confirmed the effect restrain of chain motion by fullerene.^{26,27} For the T_g decreases and the ΔC_p increases above 1.00 wt %, it may be due to the aggregation of fullerene which produced micrometer voids and led to the decrease of density, that is confirmed by the morphologies presented later. As a result, the chain mobility increased.²⁸

Dielectric Properties of PEN and PEN/Fullerene Nanocomposites

The dielectric constant (ϵ') for the PEN/fullerene nanocomposites at 1 KHz is presented in Figure 7(a). Overall, with increasing of fullerene content, the dielectric constant of these composites first decreased to the minimum, then gradually increased, and finally tends to be stable. The dielectric constant of the pure PEN is 3.51. However, when the fullerene loading is 1.50 wt %, dielectric constant of the PEN/fullerene nanocomposite is decreased to its minimum as 2.59. Then, as fullerene loading goes, the dielectric constant of the PEN/fullerene nanocomposites increased and became stable. However, they are all in the range from 3.21 to 3.26 and still smaller than that of

PEN matrix. This result conforms to reports about low-k composites by other researchers.^{15,29} It should be noted that the dielectric transition of PEN/fullerene nanocomposites once again happens about 1.50 wt % fullerene content. This point, surprisingly, is very close to rheological percolation observed above. In other words, the number of fullerene particles required to approach the dielectric transition is similarly to that required for the rheological percolation threshold. This result is different from the polymer/GN and polymer/CNT systems, for polymer/GN system the dielectric transition usually larger than the rheological percolation threshold,⁶ and for polymer/CNT system the dielectric transition usually not been observed.^{7,8}

Figure 7(b) presented the variation of the ϵ' with frequency, the dielectric constants of all the nanocomposites stably reduced with increasing frequency. Besides, it was clear that with the increasing of fullerene content, the dielectric constants at all frequencies were presented the same situation as is shown in Figure 7(a). This result is different from polymer/GN and polymer/CNT systems, for which the regulation of dielectric constant at high frequency is different from that at low frequency.^{6,30}

The dielectric constant of air was 1.00, so the hollow cage structure of the fullerene was the main reason of the reduction of dielectric constants^{9,10,15,29} while the increase of dielectric constants may be attributed to the partial fullerene aggregation.

Figure 7(c) gives the dielectric loss tangent value ($\tan \delta$) of PEN/fullerene nanocomposites at 1 K and 25°C. It can be seen that the $\tan \delta$ is in the range from 0.001 to 0.007.

Mechanical Properties of PEN and PEN/Fullerene Nanocomposites

Figure 8 shows the mechanical properties of PEN and PEN/fullerene nanocomposites. Tensile strength and tensile modulus of the pure PEN film are 73.7 MPa and 1698.1 MPa, respectively, but both of them obviously increased with the increase of fullerene loading. When fullerene loading increases to 1.50 wt %, both the tensile strength and tensile modulus reached their maximums (as 93.6 MPa and 1951.5 MPa) increased by 27% and 15% compared with those of pure PEN, respectively. Then mechanical properties of PEN/fullerene nanocomposites decreased with the increase of fullerene content, and finally they both tend to be stable, but they are still higher than the pure PEN.

The mechanical performances such as tensile strength and tensile modulus of the polymer-based nanocomposites depend on the filler dispersion and interfacial interaction.³¹ The dispersion of fullerene that restricted the mobility of PEN polymer chains improved the tensile modulus and the strength in the low content. This kind of reinforcement effect achieved the strongest at 1.50 wt % fullerene loading where a rheological percolation network structure formed. However, the lessening of strength with higher fullerene content may be ascribed to the bad dispersion of fullerene in higher loading systems. Figure 8 also shows that the elongation steadily decreases from 8.86% to 6.53% with the increasing fullerene content, this once again indicates that the existence of fullerene have effectively restricted the movement of PEN chains.^{32,33}

Morphological of PEN and PEN/Fullerene Nanocomposites

Figure 9 shows the SEM pictures of fractured morphologies of pure PEN and PEN/fullerene nanocomposites, Figure 9(a) exhibits that the surface of PEN is relatively smooth. However, the addition of fullerene increases fracture surface. It is found that the separate fullerene aggregated to fullerene bundle in PEN/fullerene nanocomposites, even in the PEN/fullerene0.5 nanocomposite shown in Figure 9(b). Researchers have found that fullerene had a very strong aggregate trend to form fullerene bundle at a very low concentration, the size of fullerene bundle is dependent on fullerene loading.^{15,34–37} Clearly, as is shown in Figure 9(c,d), the size of fullerene bundle in PEN/fullerene1.5 nanocomposite (about 1.2 μm) is smaller than that in PEN/fullerene3.0 (about 2.5 μm). There are micrometer voids in samples with fullerene containing above 1.50 wt %, but not obvious in samples with fullerene containing below 1.50 wt %, those micrometer voids may also affect the decrease in the dielectric constant. And obviously the micrometer voids are between the fullerene bundle and PEN matrix, shows a herringbone interconnection of the matrix, this phenomenon has also been reported by others.³⁸ This may be explained by the formation of organic microcrystals,^{39,40} at the mixed solution step of

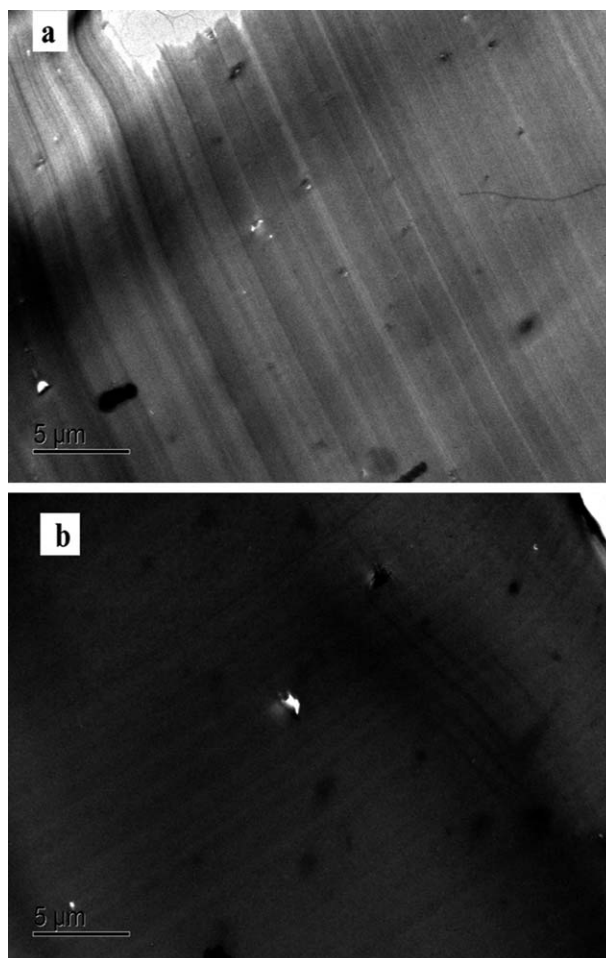


Figure 10. TEM pictures of (a) PEN/Fullerene0.5 and (b) PEN/Fullerene2.0.

preparing the nanocomposites, when the concentration of fullerene reaches the saturation point, the crystallization process takes place and fullerene microcrystals are formed.³⁹

As considered to be a powerful tool for studies on morphology,⁴¹ TEM can give us a better understanding of the size and dispersion of fullerene bundles in PEN matrix,³⁹ the TEM pictures of PEN/Fullerene nanocomposites are shown in Figure 10, the dark regions correspond to fullerene bundles.^{41–43} Figure 10(a) showed the size of fullerene bundles in PEN/Fullerene0.5 is about 0.5 μm and dispersed evenly, but in Figure 10(b) fullerene bundles in PEN/Fullerene2.0 is about 2.5 μm and the dispersion becomes very bad. This result conforms to the SEM pictures.

CONCLUSIONS

In this study, the PEN/fullerene nanocomposites were prepared by one solution-cast method via continuous supersonic technology, and the rheological, dielectric, mechanical properties, and morphological were investigated. The rheological test shows that at low frequencies PEN/fullerene nanocomposites experienced a transition from liquid-like behavior to solid-like one with the increasing of fullerene loading, besides a rheological percolation network structure formed and highly hinders the large scale

motion of polymer chains when the fullerene loading reached 1.50 wt %, that is confirmed by DSC. Meanwhile, at this loading level a dielectric transition occurs, and the mechanical property also showed the best performance. The fitted rheological percolation threshold is about 1.55 wt %, which is very close to the experimental observations. The SEM and TEM tests showed fullerene aggregated to fullerene bundles and the dispersion of the bundles becomes bad when the fullerene content exceed 1.50 wt %. This work not only presented a relationship between structure (dispersion, interaction, percolation) and properties, but also shows that the rheological percolation threshold is close to dielectric transition value in the spherical filler low dielectric constant polymer material, this study have both academic and practical values.

REFERENCES

1. Seyhan, A. T.; Gojny, F. H.; Tanoglu, M.; Schulte, K. *Eur. Polym. J.* **2007**, *43*, 2836.
2. Gojny, F. H.; Schulte, K. *Compos. Sci. Technol.* **2004**, *34*, 2303.
3. Gojny, F. H.; Wichmann, M.; Fiedler, B.; Schulte, K. *Compos. Sci. Technol.* **2005**, *65*, 2300.
4. Gojny, F. H.; Nastalczyk, J.; Roslaniec, Z.; Schulte, K. *Chem. Phys. Lett.* **2003**, *370*, 820.
5. Takahashi, T.; Kato, H.; Ma, S. P.; Sasaki, T.; Sakurai, K. *Polymer* **1995**, *36*, 3803.
6. Samaneh, A.; Pierre, J.; Carreau Abdesslem, D.; Michel, M. *Rheologica Acta* **2009**, *9*, 943.
7. Fan, P.; Wang, L.; Yang, Y. T.; Chen, F.; Zhong, M. Q. *Nanotechnology* **2012**, *23*, 365702.
8. Kalgaonkar, A. R.; Jog, P. *J. Polym. Int.* **2008**, *57*, 114.
9. Hermann, H.; Zagorodniy, K.; Touzic, A.; Taut, M.; Seifert, G. *Microelectron Eng.* **2005**, *82*, 387.
10. Wang, Y. K.; Seifert, G.; Hermann, H. *Phys. Stat. Sol.* **2006**, *15*, 3868.
11. Zhan, Y. Q.; Lei, Y. J.; Meng, F.; Zhong, J. C.; Zhao, R.; Liu, X. B. *J. Mater. Sci.* **2011**, *46*, 824.
12. Saxena, A.; Sadhana, R.; Rao, V. L.; Kanakavel, M.; Ninan, K. N. *Polym. Bull.* **2003**, *50*, 219.
13. Takahashi, T.; Kato, H.; Ma, S. P.; Sasaki, T.; Sakurai, K. *Polymer* **1995**, *36*, 3803.
14. Zhan, Y. Q.; Yang, X. L.; Meng, F. B.; Lei, Y. J.; Zhong, J. C.; Zhao, R.; Liu, X. B. *Polym. Int.* **2011**, *60*, 1342.
15. Chen, Y. W.; Zhong, J. C.; Wang, D. Y.; Liu, M.; Liu, X. B. *J. Mater. Sci.: Mater. Electron.* **2011**, *22*, 304.
16. Aranguren, M. I. *Polymer* **1998**, *39*, 4897.
17. Zhan, Y. Q.; Meng, F. B.; Yang, X. L.; Wei, J. J.; Yang, J.; Zou, Y. K.; Guo, H.; Zhao, R.; Liu, X. B. *J. Appl. Polym. Sci.* **2013**, *127*, 1827.
18. Yang, X. L.; Zhan, Y. Q.; Zhao, R.; Liu, X. B. *J. Appl. Polym. Sci.* **2012**, *124*, 1723.
19. Wang, J. W.; Wu, C. C.; Liu, R. N.; Li, S. Q. *Polym. Bull.* **2013**, *70*, 1327.
20. Yang, X. L.; Wang, Z. C.; Zhan, Y. Q.; Yang, J.; Zou, Y. K.; Zhao, R.; Liu, X. B. *Polym. Int.* **2013**, *62*, 629.
21. Aranguren, M. I. *Polymer* **1998**, *39*, 4897.
22. Wu, D. F.; Wu, L.; Zhang, M.; Zhao, Y. L. *Polym. Degrad. Stabil.* **2008**, *93*, 1577.
23. Wu, D. F.; Zhang, Y. S. *J. Appl. Polym. Sci.* **2008**, *108*, 1934.
24. Sara, S. A.; Naghmeh, F.; Milad, M. *Polym. Test.* **2012**, *3*, 671.
25. Zhan, Y. Q.; Lei, Y. J.; Meng, F. B.; Zhong, J. C.; Zhao, R.; Liu, X. B. *J. Mater. Sci.* **2011**, *46*, 824.
26. Richard, A. V.; Bryan, B. S.; Oliver, K. T.; Emmanuel, P. G. *J. Polym. Sci.: Part B: Polym. Phys.* **1997**, *35*, 59.
27. Cheng Stephen, Z. D.; Cao, M. Y.; Wunderlich, B. *Macromolecules* **1986**, *19*, 1868.
28. Lee, J. Y.; Kristin, E. S.; Edwin, P. C.; Zhang, Q. L.; Emrick, T.; Alfred, J. C. *Macromolecules* **2007**, *40*, 7755.
29. Yuan, Y.; Lin, B. P.; Sun, Y. M. *J. Appl. Polym. Sci.* **2011**, *120*, 1133.
30. Wang, B. H.; Liang, G. Z.; Jiao, Y. C.; Gu, A. J.; Liu, L. M.; Yuan, L.; Zhang, W. *Carbon* **2013**, *54*, 224.
31. Prashantha, K.; Soulestin, J.; Lacrampe, M. F.; Claes, M.; Dupin, G.; Krawczak, P. *Exp. Polym. Lett.* **2008**, *10*, 735.
32. Tang, H.; Ma, Z.; Zhong, J.; Yang, J.; Zhao, R.; Liu, X. B. *Colloids Surf. A* **2011**, *384*, 311.
33. Sandler, J.; Broza, G.; Nolte, M.; Schulte, K.; Lam, Y. M.; Shaffer, M. S. P. *Sci. B* **2003**, *42*, 479.
34. Bulavin, L. A.; Adamenko, I. I.; Yashchuk, V. M.; Ogul'chansky, T. Y.; Prylutsky, Y. I.; Durov, S. S.; Scharff, P., et al. *J. Mol. Liquids* **2001**, *93*, 187.
35. Bezmelnitsyn, V. N.; Eletsky, A. V.; Okun, M. V. *Phys. Usp* **1998**, *41*, 1091.
36. Lu, Z.; He, C.; Chuang, T. S. *Polymer* **2001**, *42*, 5233.
37. Calleja, F. J. B.; Giri, L.; Asano, T.; Mieno, T.; Sakurai, A.; Ohnuma, M.; Sawatari, C. *J. Mater. Sci.* **1996**, *31*, 5153.
38. Adam, J. M.; Klaus, M. *Advise Mater.* **2008**, *20*, 240.
39. Kasai, H.; Oikawa, H.; Okada, S.; Nakanishi, H. B. *Chem. Soc. Jpn.* **1998**, *71*, 2597.
40. Kai, L. C.; Menachem, E. *Langmuir* **2006**, *22*, 10994.
41. Markus, H.; Ilka, K.; Enrico, D. C. *Adv. Funct. Mater.* **2009**, *19*, 3662.
42. Ari, L.; Majumdar, H. S.; Baral, J. K.; Jansson, F.; Österbacka, R.; Ikkala, O. *Appl. Phys. Lett.* **2008**, *93*, 203309.
43. Giacalone, F.; Mart, N. *Chem. Rev.* **2006**, *106*, 5136.